Table I

Devices turn on parameter of different grain size and film quality.

	Grain Size				
6/30 (*μm/μm*)	**ELA 0.3**	**SSL 1**	**SSL 0.9**	**SSL 0.3**	**SSL 0.1**
***Mobility μ* (*cm²/V-s*)**	**176**	**229**	**218**	**138**	**35**
***Threshould Voltage Vt* (*V*)**	**1.2**	**0.5**	**0.5**	**0.7**	**2.4**
***Subthreshould swing S.S* (*V/decade*)**	**0.48**	**0.3**	**0.25**	**0.425**	**0.95**

ELA and SSL Sample are W/L= 6/30 (*μm*)

Table II

γ Value for different grain growth conditions.

Laser Type	**ELA**	**SSL**					
Thickness (*nm*)	50	50				100	
Laser Energy Density (mJ/cm^2)	380	530	507	461	438	576	553
γ	1.55	2	2	1.5	1	2	2

ELA and SSL Sample are W/L= 6/30 (μm)

Table Ⅲ

Trap state density with different grain size.

			Trap State Density (cm^{-2})	
Laser type	Laser Energy Density (mJ/cm^2)	Grain size (μm)	W/L= 6/30 (μm)	W/L= 6/12 (μm)
ELA	380	0.3	1.56×10^{12}	1.70×10^{12}
SSL	507	1	1.24×10^{12}	1.18×10^{12}
	484	0.7	1.36×10^{12}	1.23×10^{12}
	437	0.55	1.55×10^{12}	1.51×10^{12}
	414	0.3	1.68×10^{12}	1.89×10^{12}
	391	0.1	2.69×10^{12}	2.90×10^{12}

ELA and SSL Sample are W/L= 6/30 (μm)

Table IV

Radiant Flux Intensity (*Watt*) of RGB-LED

	Luminance (*nits*)	Radiance Flux(*mWatt*)	Luminance (%)	Radiance Flux (%)
White	4670	3.49		
Red	1172	1.32	**25.1**	37.7
Green	3176	1.17	**68**	33.6
Blue	321	1	**6.9**	28.7

Table V

Absorptivity of R, G, B light, and poly-Si film thickness = 50*nm*

Wavelength (*nm*)	Absorptance Coefficient (cm^{-1})	Absorptivity (Ratio)	*Ip*($10^{-12}A$) Grain Size =1(μm)
633	6489	1	1.84
539	18869	4.7	3.11
453	63099	29.7	9.44

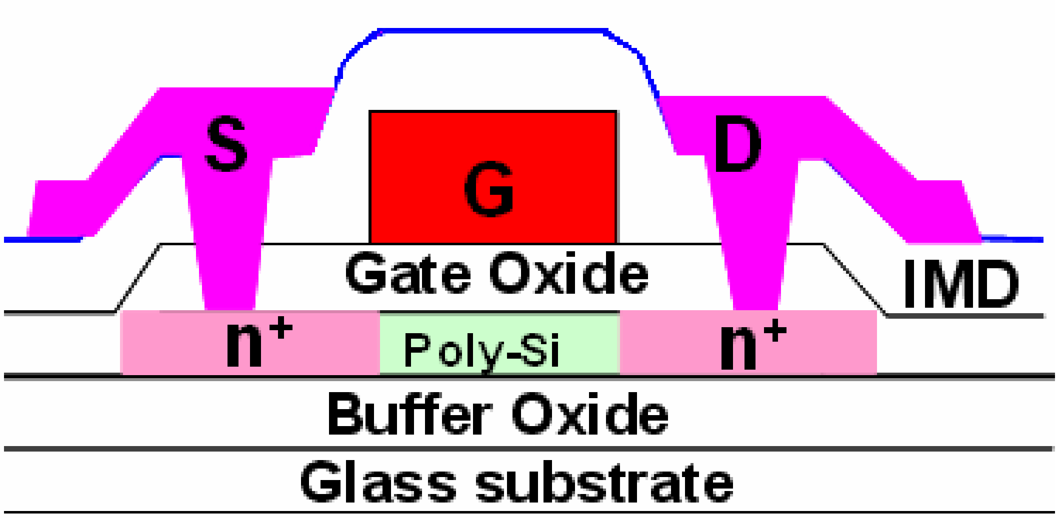

Fig.2-1. Schematic cross-sectional view of poly-Si TFT.

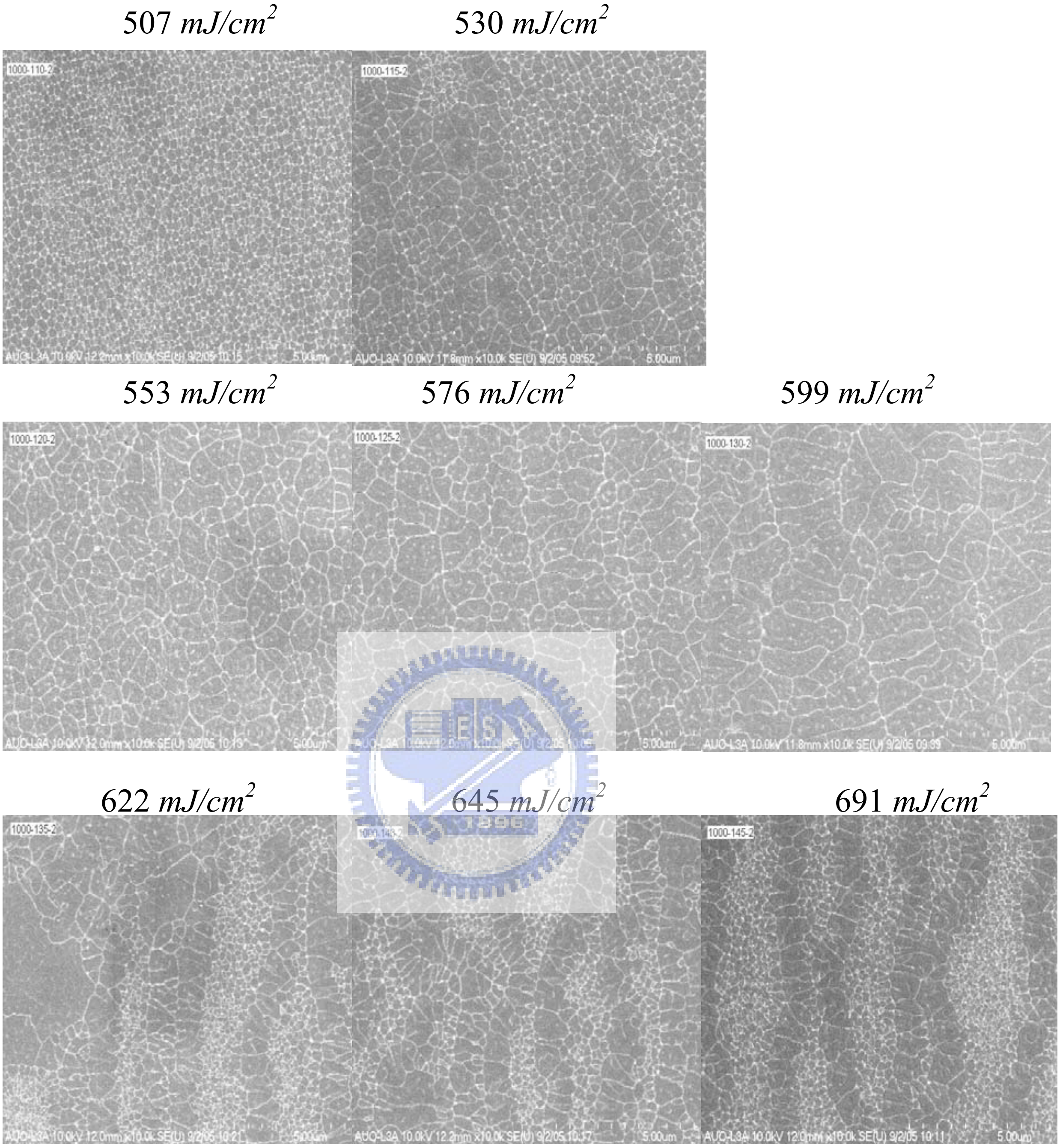

Fig. 2-3 SEM image of different laser energy density in the channel thickness of 100*nm*.

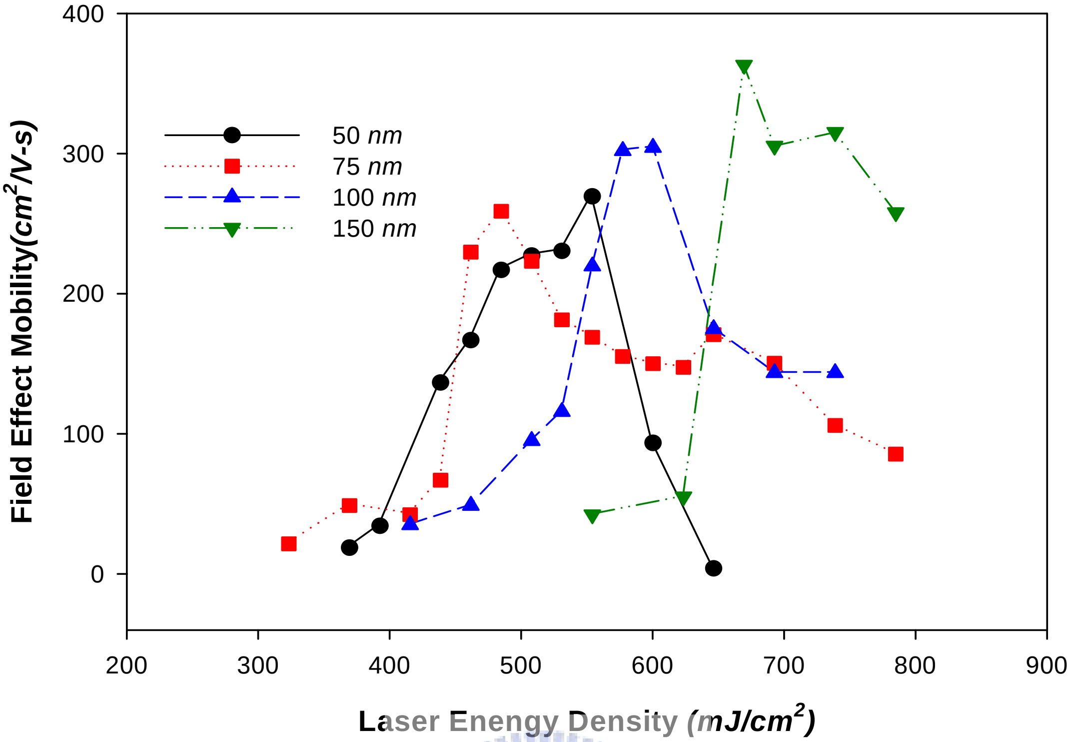

Fig.2-4-1(a) Process window of field effect mobility with different channel thickness utilizing solid state laser crystallization ($W/L = 6\mu m$ / 30 μm).

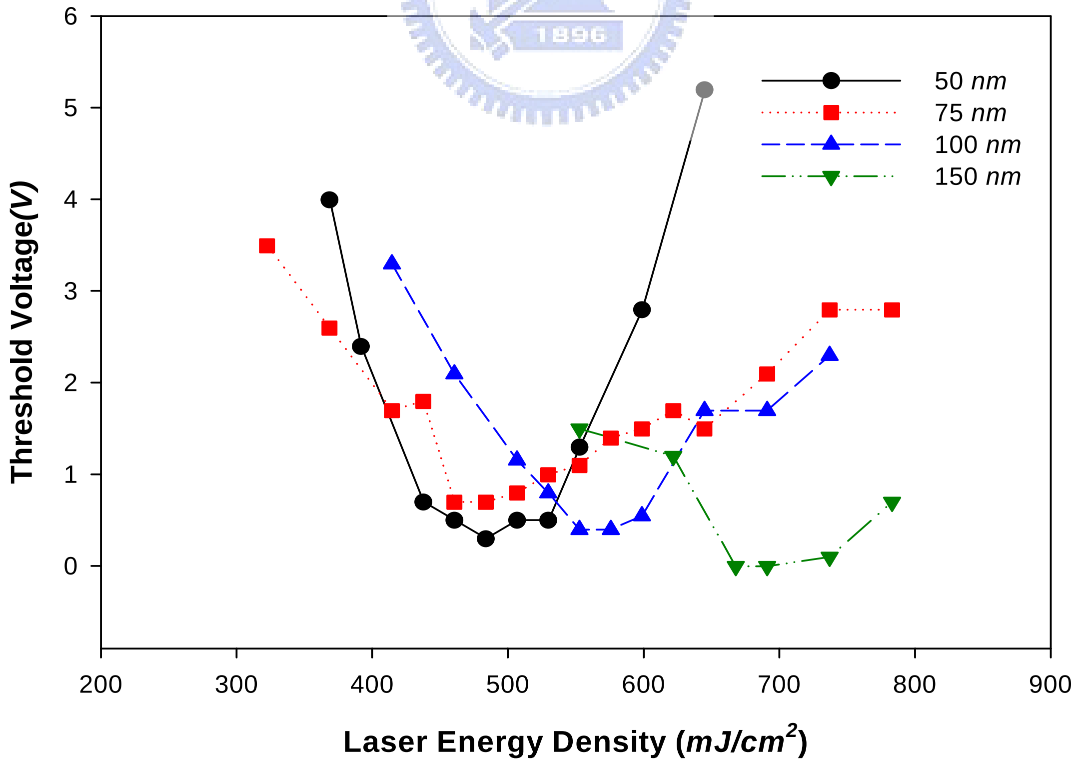

Fig2-4-1(b) Process window of threshold voltage with different channel thickness utilizing solid state laser crystallization ($W/L = 6\mu m$ / 30 μm).

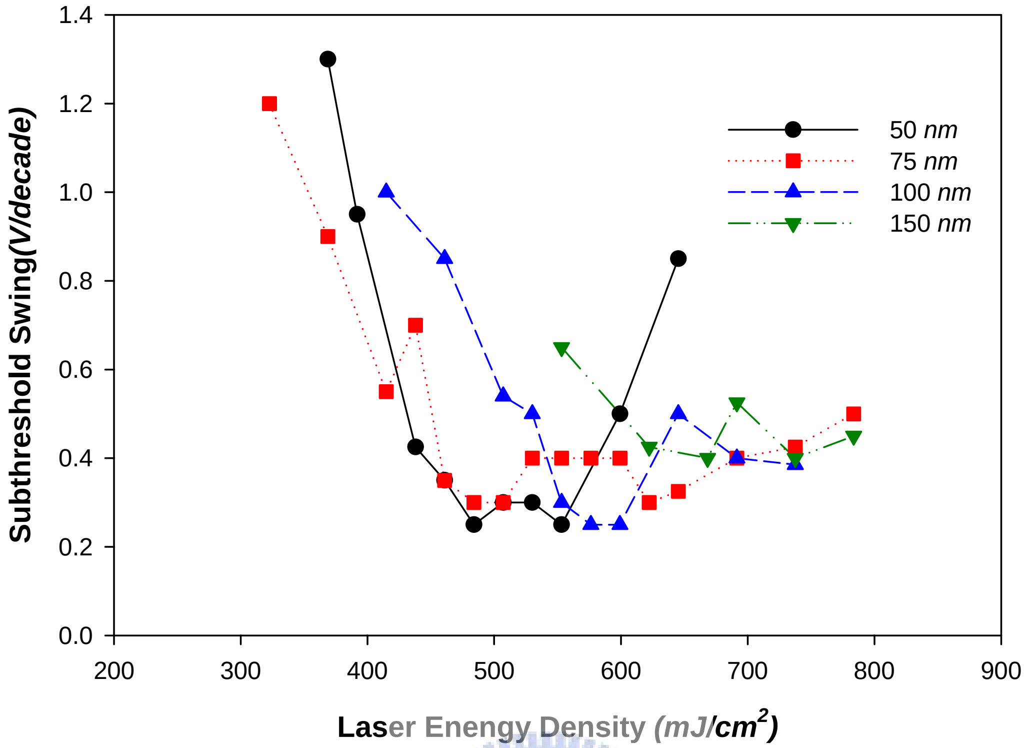

Fig2-4-1(c) Process windows of subthreshold swing with different channel thickness utilizing solid state laser crystallization (W/L = 6μm / 30 μm).

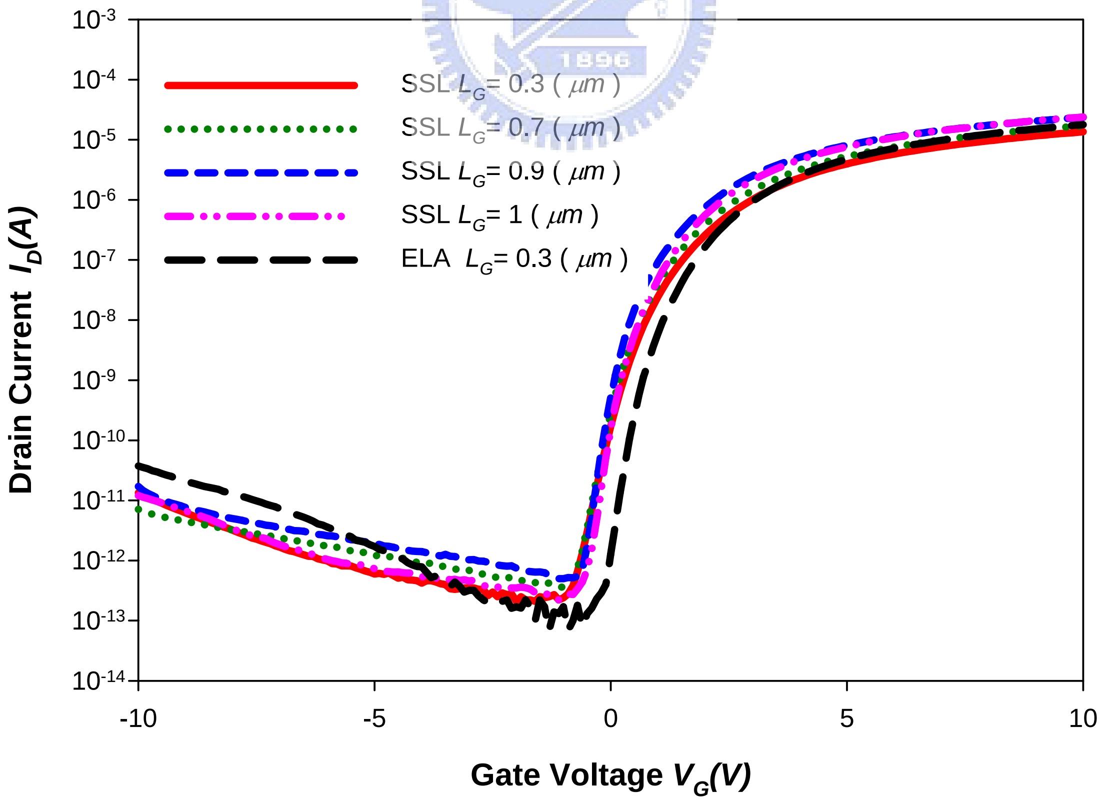

Fig.2-4-3(a) Transfer characteristics of different grain size and film quality for V_{DS}=2.1V (W/L = 6μm / 30 μm).

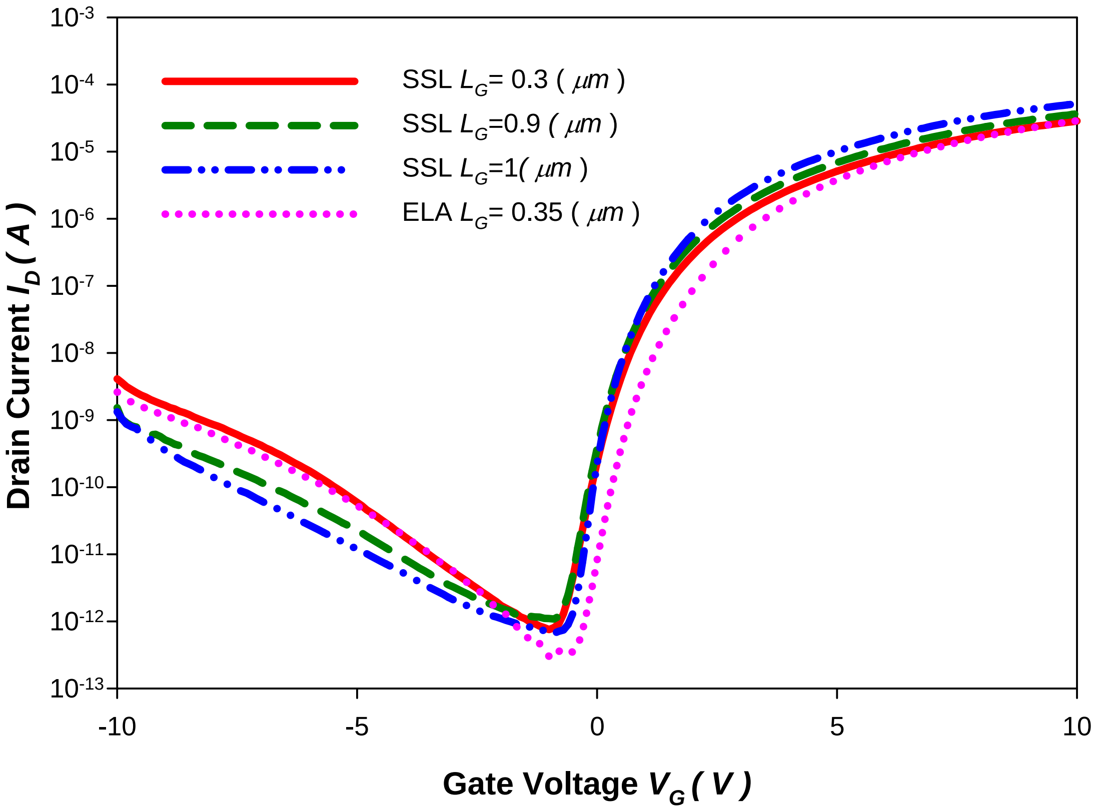

Fig.2-4-3(b) Transfer characteristics of different grain size and film quality for V_{DS}= 6.1 V (W/L = 6μm / 30 μm).

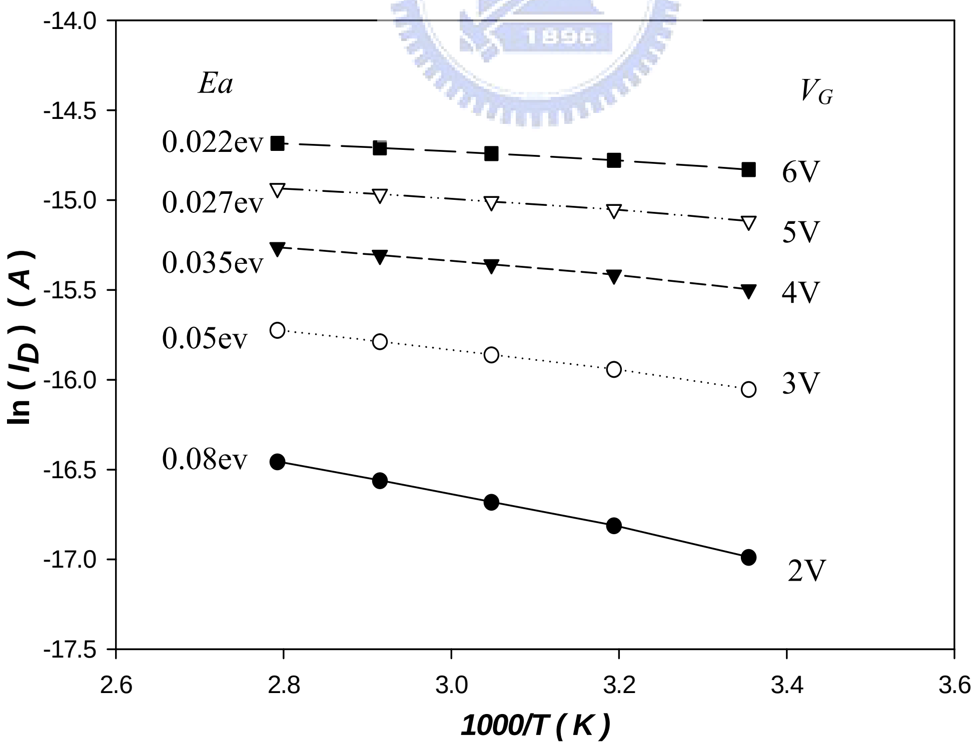

Fig.2-5-1 Arrhenius plot of the drain current of W/L = 6μm / 30 μm n-channel device for different drain voltages. The slope of each line defines the activation energy (E_a).

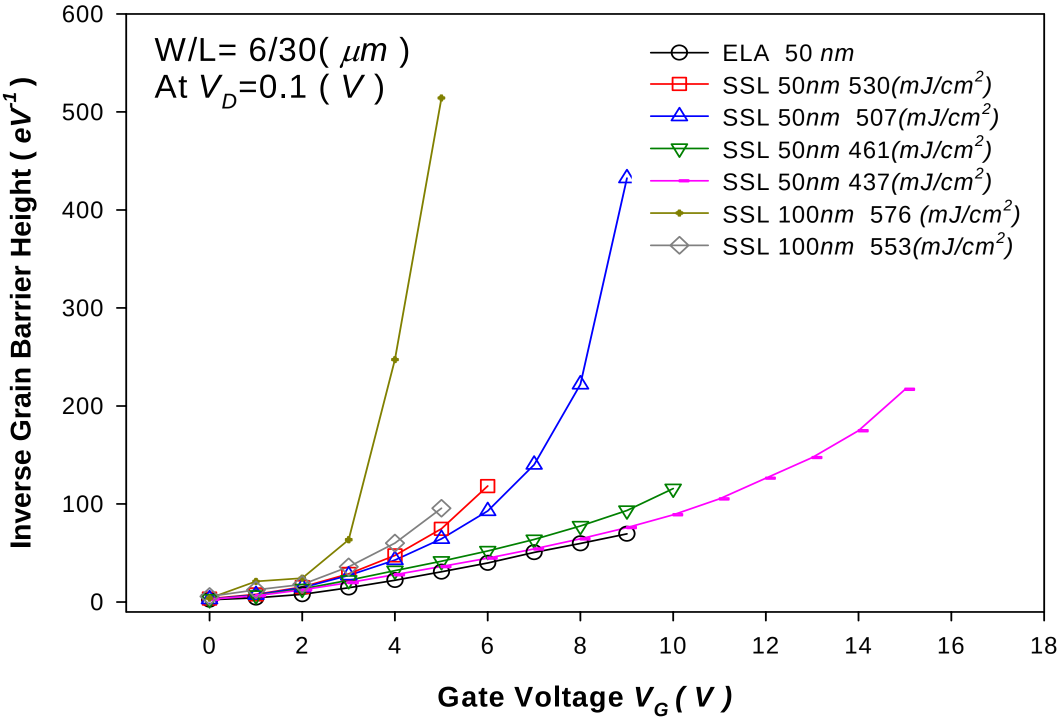

Fig. 2-5-2 The experimental inverse of grain barrier height versus the gate voltage for different grain growth conditions.

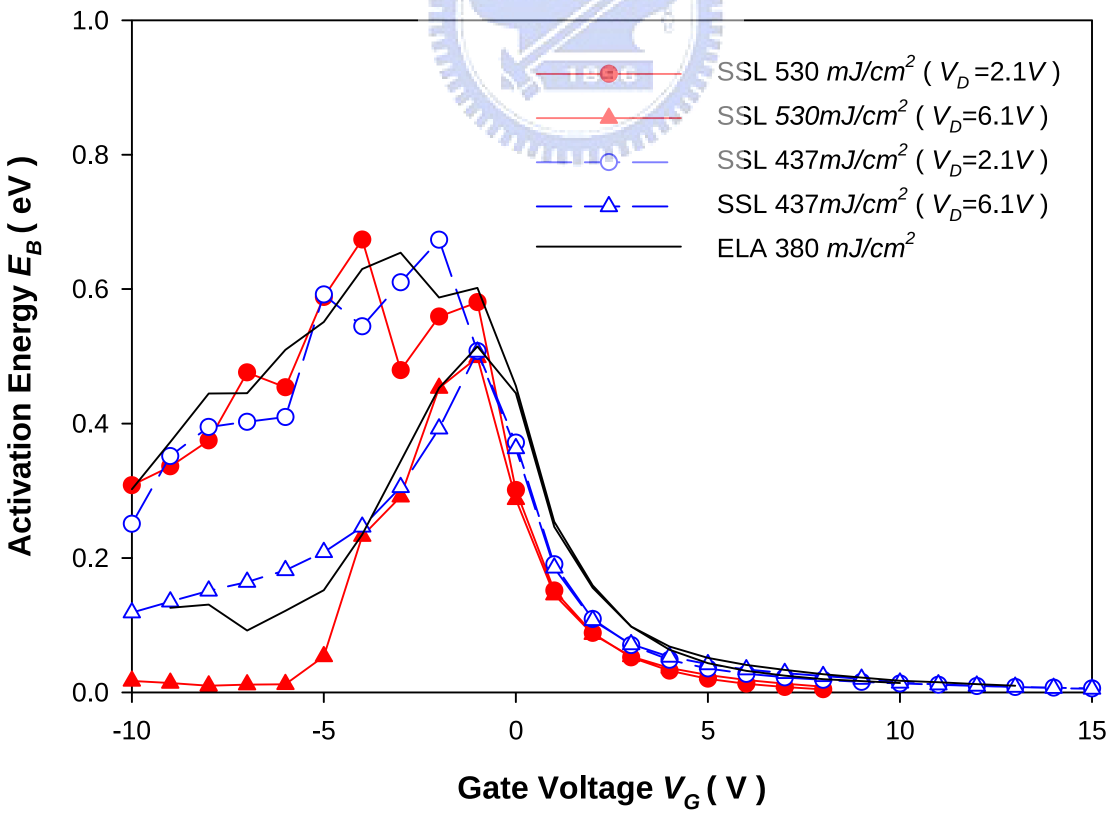

Fig. 2-5-3 The relationship of activation energy with different grain size and film quality ($W/L = 6\mu m$ / $30\ \mu m$).

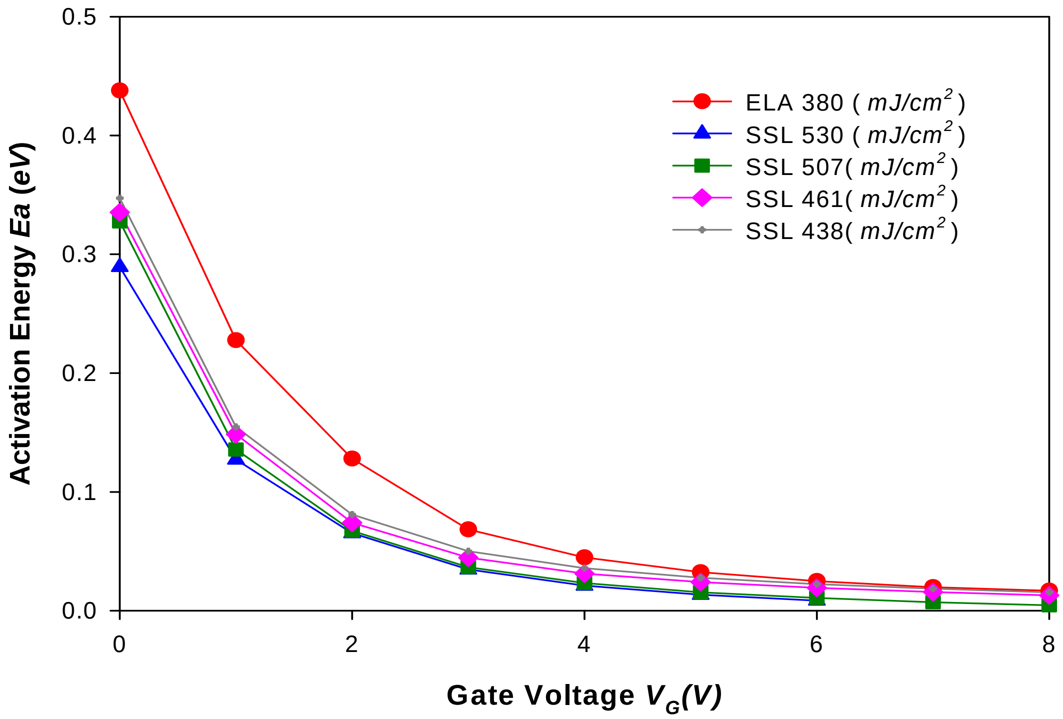

Fig. 2-5-4 The relationship of activation energy with different grain size and film quality at the channel for V_{DS}=0.1V (W/L = 6μm / 30 μm).

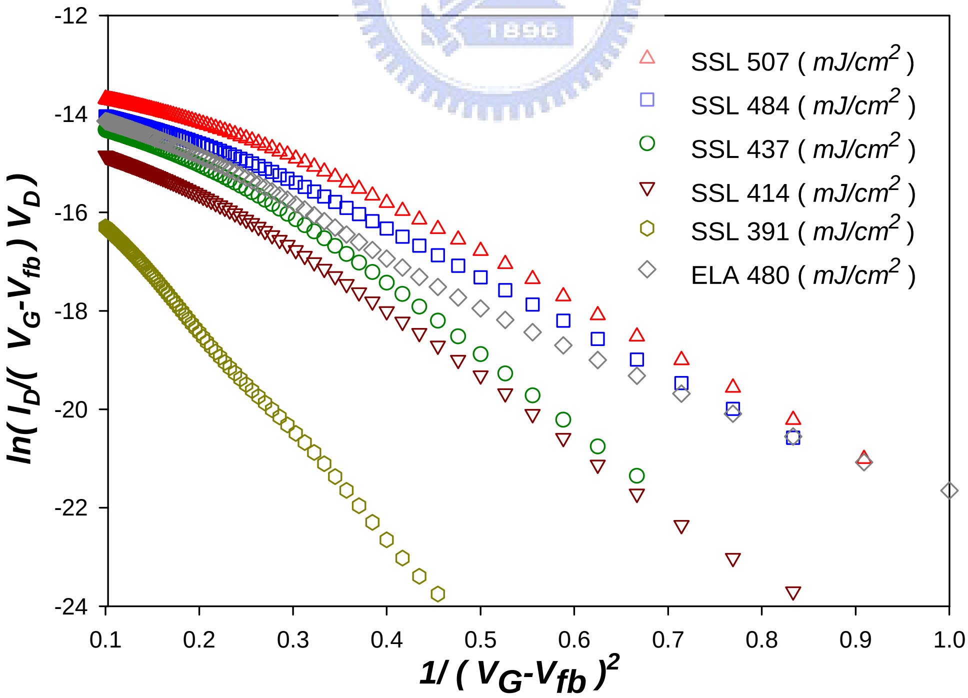

Fig. 2-5-5 Plot of ln [I_{DS}/ (V_G-V_{FB})V_{DS}] against both 1/ (V_G-V_{FB})^2, used to determine Nt at the different grain size and the film quality (W/L = 6μm / 30 μm).

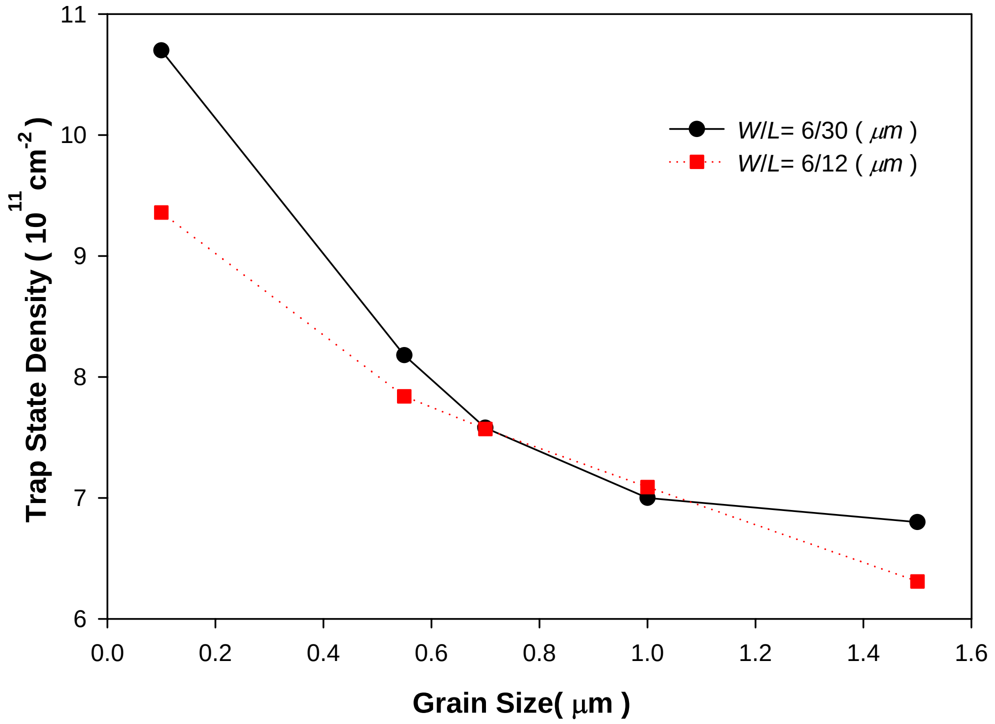

Fig. 2-5-6 Trap State Density utilizing the solid state laser to crystallization with the different grain size and different dimension.

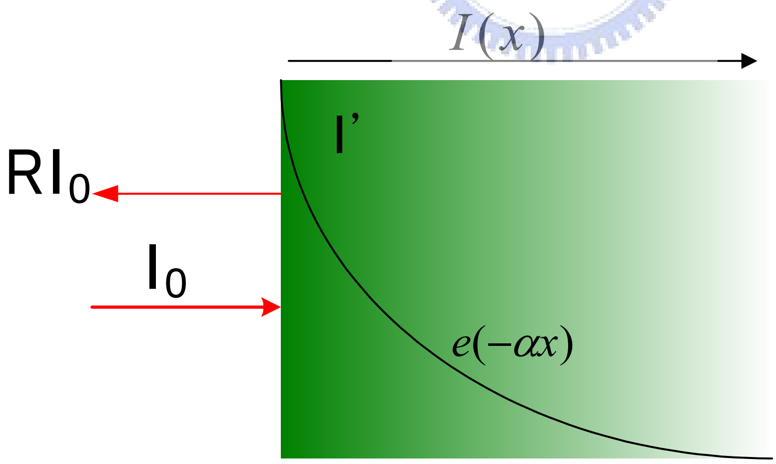

Fig. 3-1 Incident photon intensity distribution as the thickness variation.

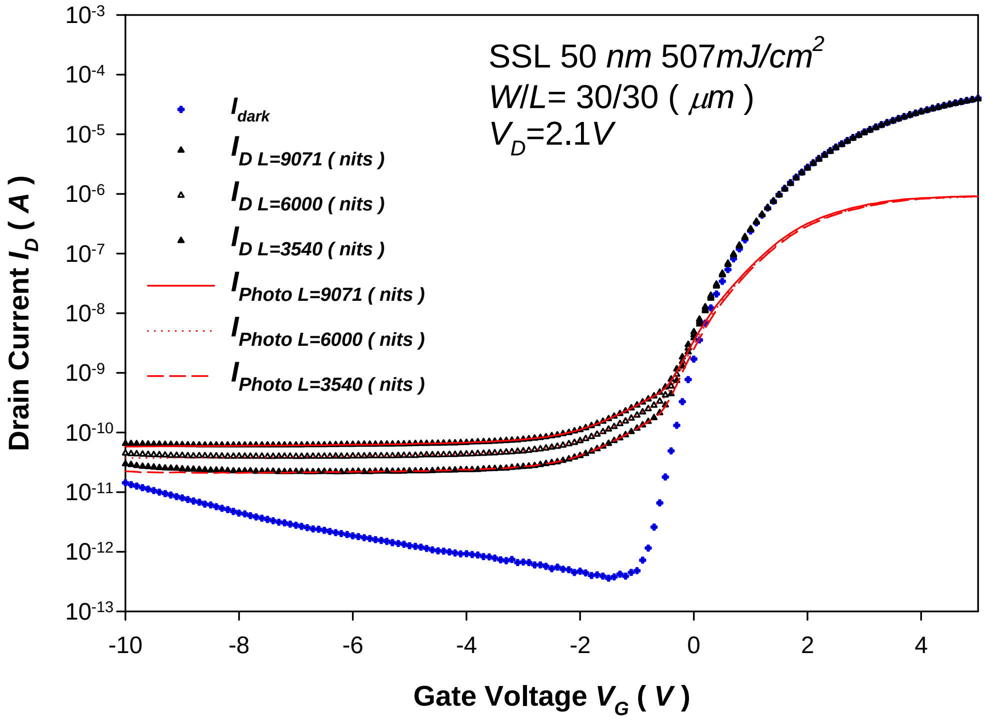

Fig. 3-2 Characteristics of drain current with various illumination of poly-Si TFTs. SSL device with the channel thickness 50*nm* and grain size *1μm* at the $V_{DS}=2.1V$.

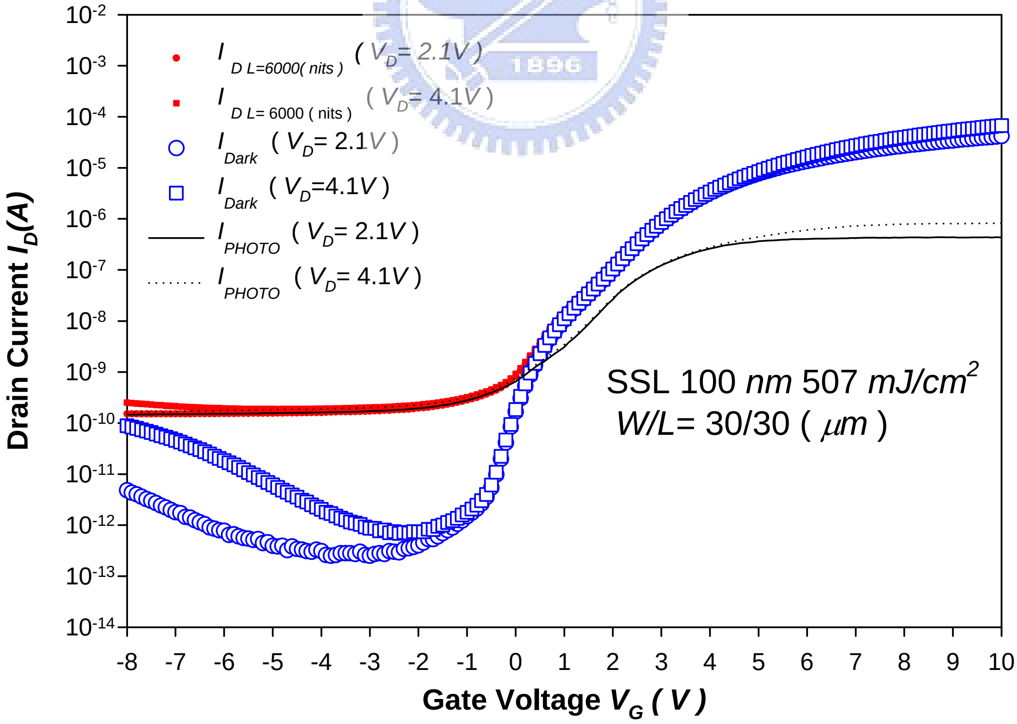

Fig. 3-3 Characteristics of drain current with illumination of 6000 (cd/m^2). SSL device with the channel thickness 100*nm* and grain size *0.3μm* at the $V_{DS}=2.1V$ and $V_{GS}= -3\ V$.

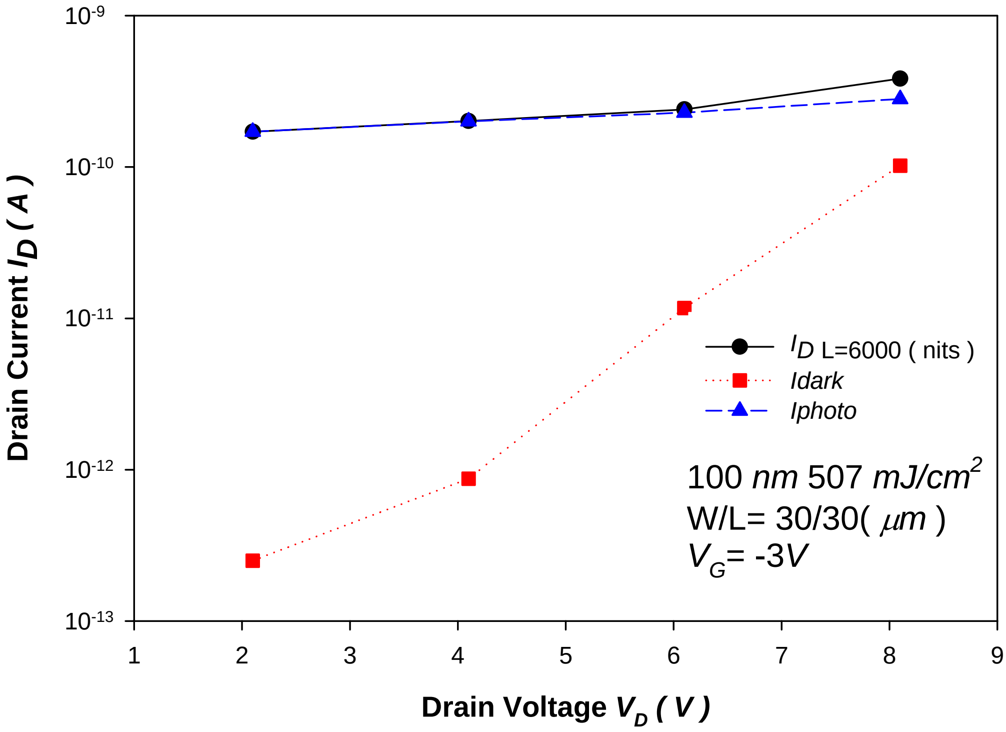

Fig.3-4 Characteristics of drain current with the illumination of 6000 (cd/m^2). SSL device with the channel thickness 100*nm* and grain size *0.3μm* at the $V_{DS}=2.1V$ and $V_{GS}= -3\ V$.

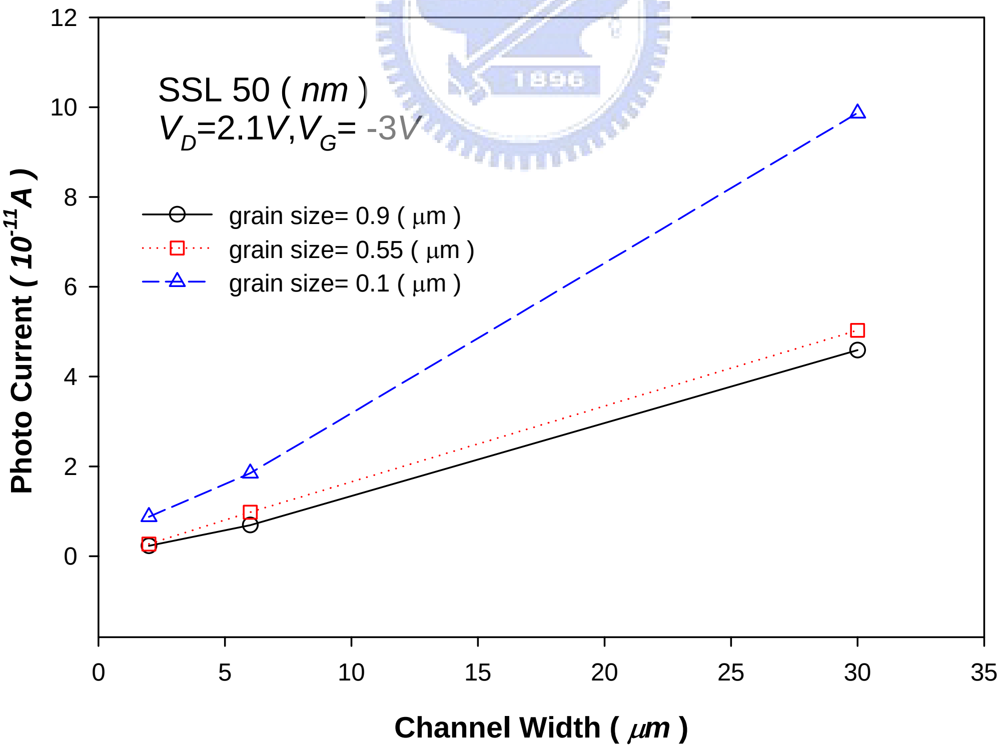

Fig. 3-5 Dependence of photo leakage current with different channel width at the channel length 6 *μm*. SSL device with the channel thickness 50*nm* at the $V_{DS}=2.1V$ and $V_{GS}= -3\ V$.

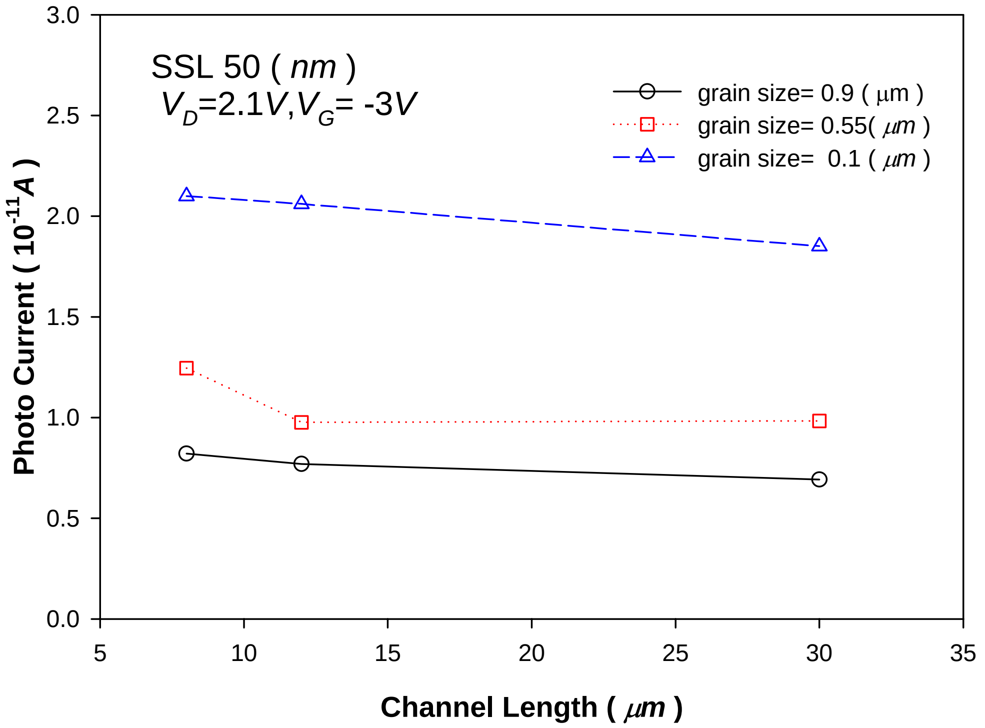

Fig. 3-6 Dependence of photo leakage current with different channel length at the channel width 6 *µm*. SSL device with the channel thickness 50*nm* at the $V_{DS}=2.1V$ and $V_{GS}= -3\ V$.

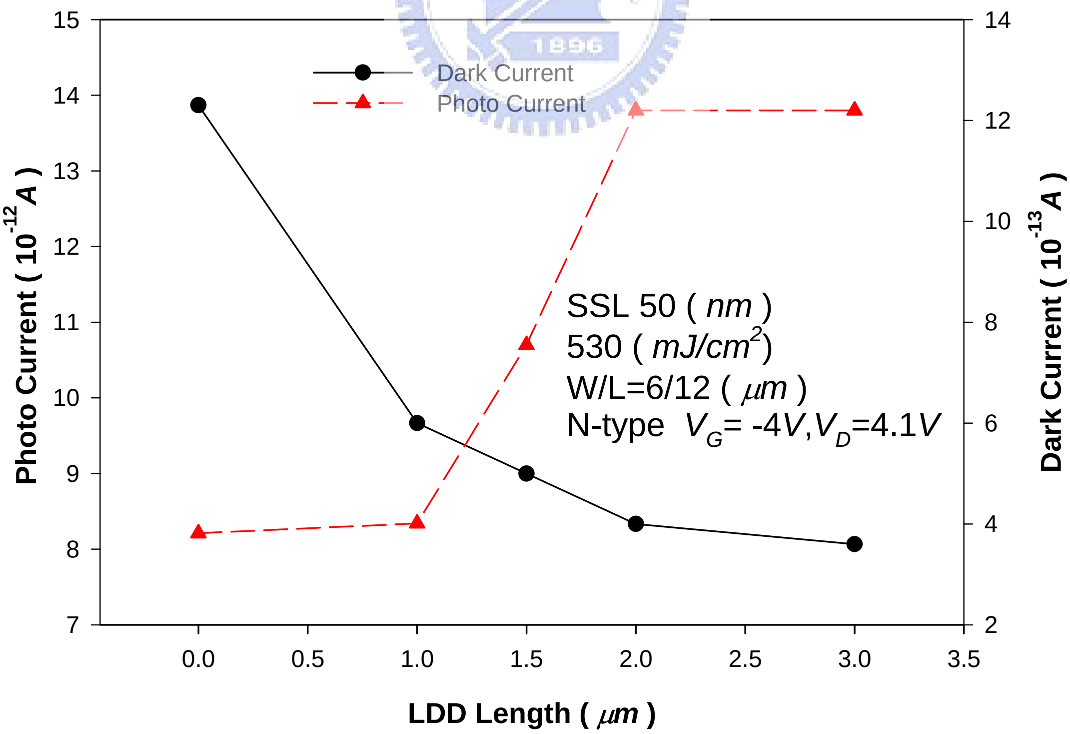

Fig. 3-7 Dependence of the photo leakage current on various LDD lengths. SSL device with the channel thickness 50*nm* at the $V_{DS}=4.1V$ and $V_{GS}= -4\ V$ ($W/L=30$ *µm/30 µm*).

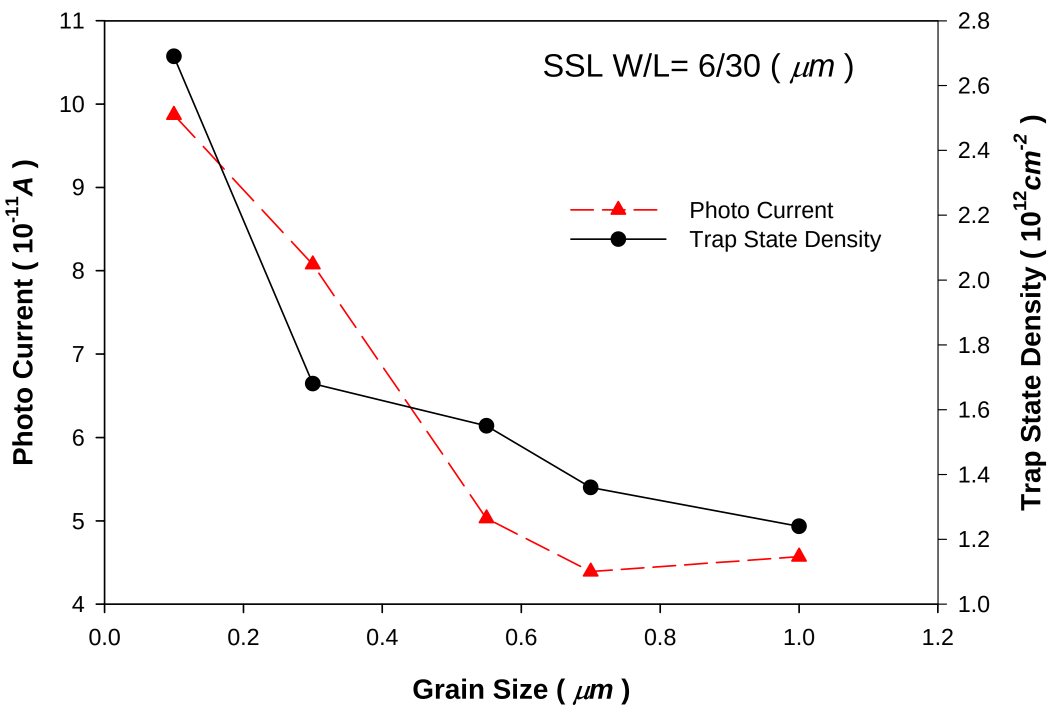

Fig. 3-8 Dependence of photo leakage current on the different grain size with the illumination of 6000 (cd/m^2). SSL device with the channel thickness 50*nm* at the V_{DS}=2.1*V* and V_{GS}= -3 *V* (*W /L=30 μm/30 μm*).

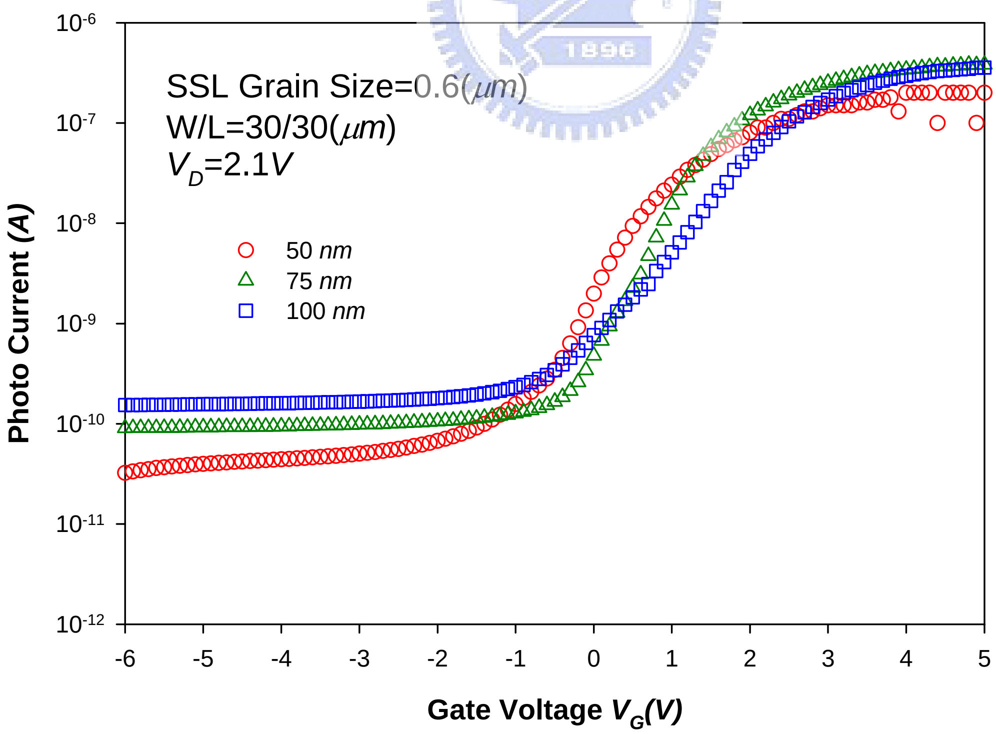

Fig. 3-9 Dependence of the photo leakage current on the different channel thickness with the illumination of 6000 (cd/m^2). SSL device with the grain size 0.6μ*m* at the V_{DS}=2.1*V* (*W /L=30 μm/30 μm*).

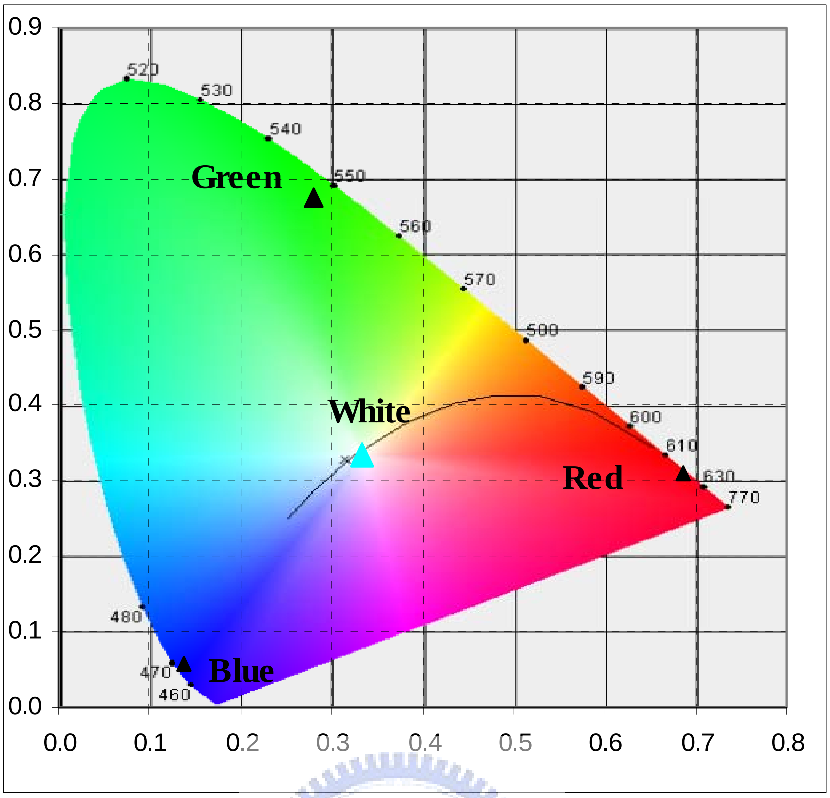

Fig. 3-10 Color coordinate of RGB-LED.

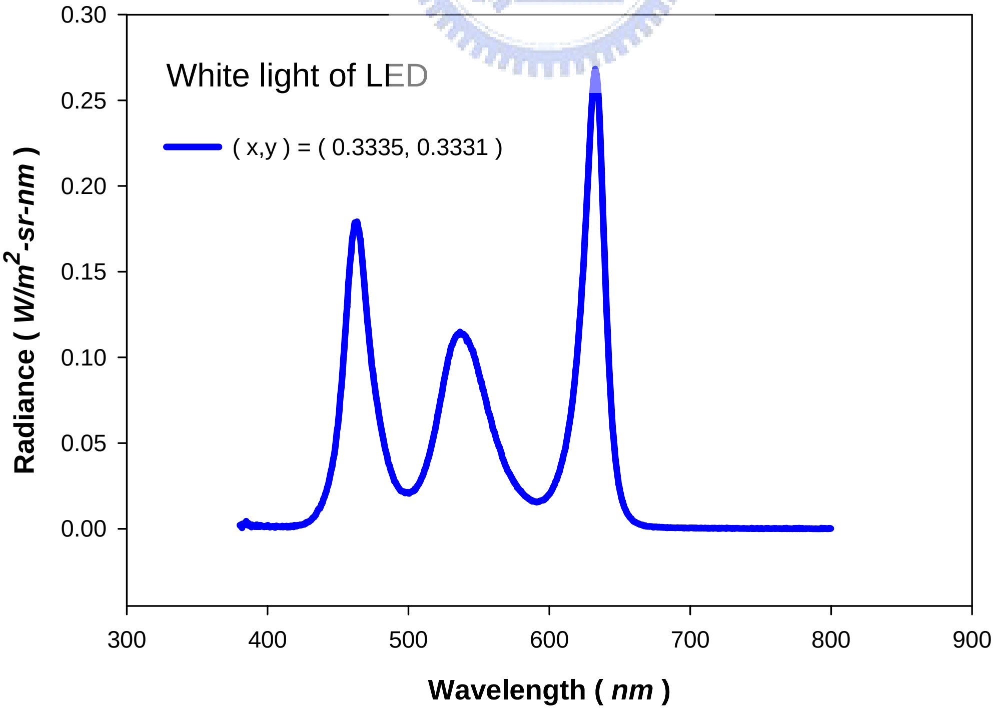

Fig. 3-11 Wavelength characteristics of white light LED.

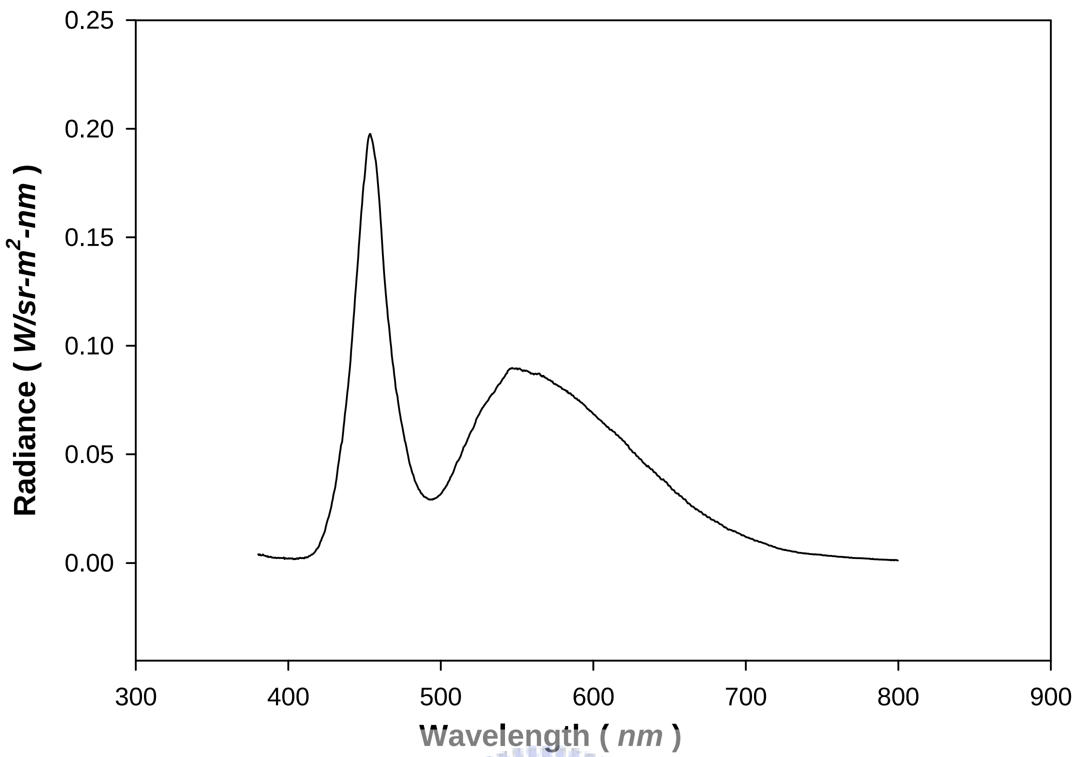

Fig. 3-12 Wavelength characteristic of CCFL backlight.

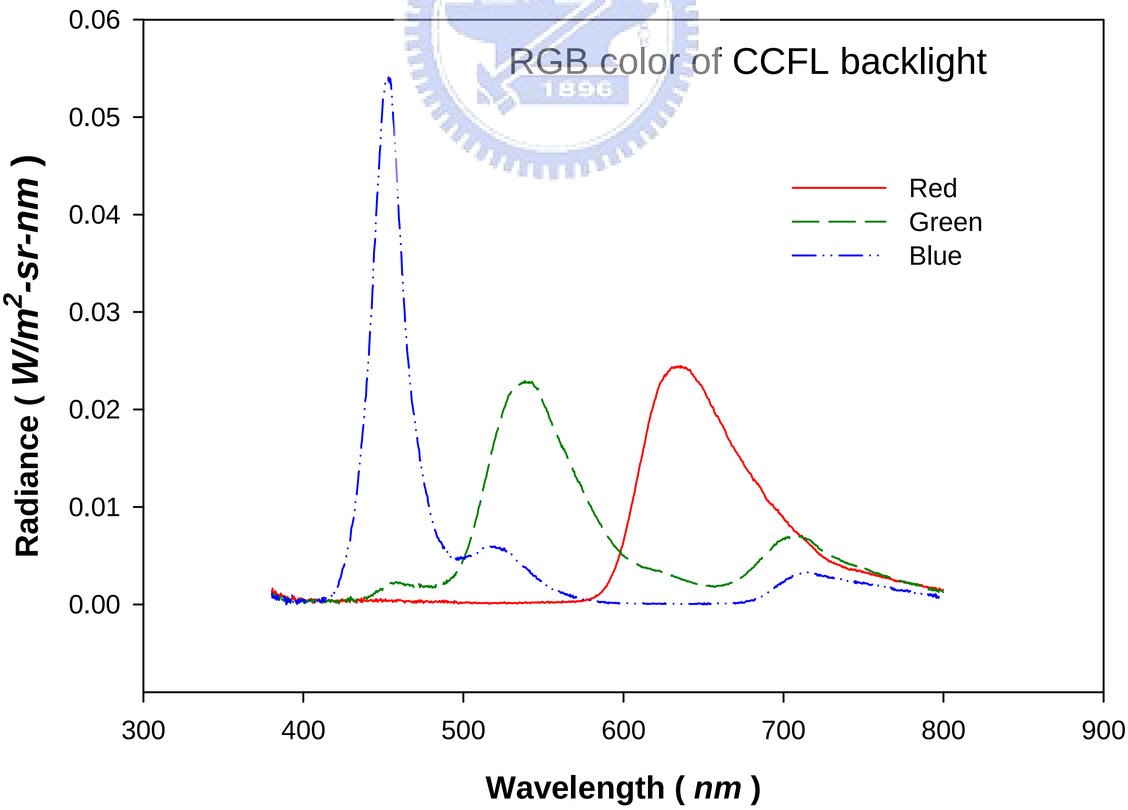

Fig. 3-13 Wavelength characteristic of CCFL backlight with the RGB filter.

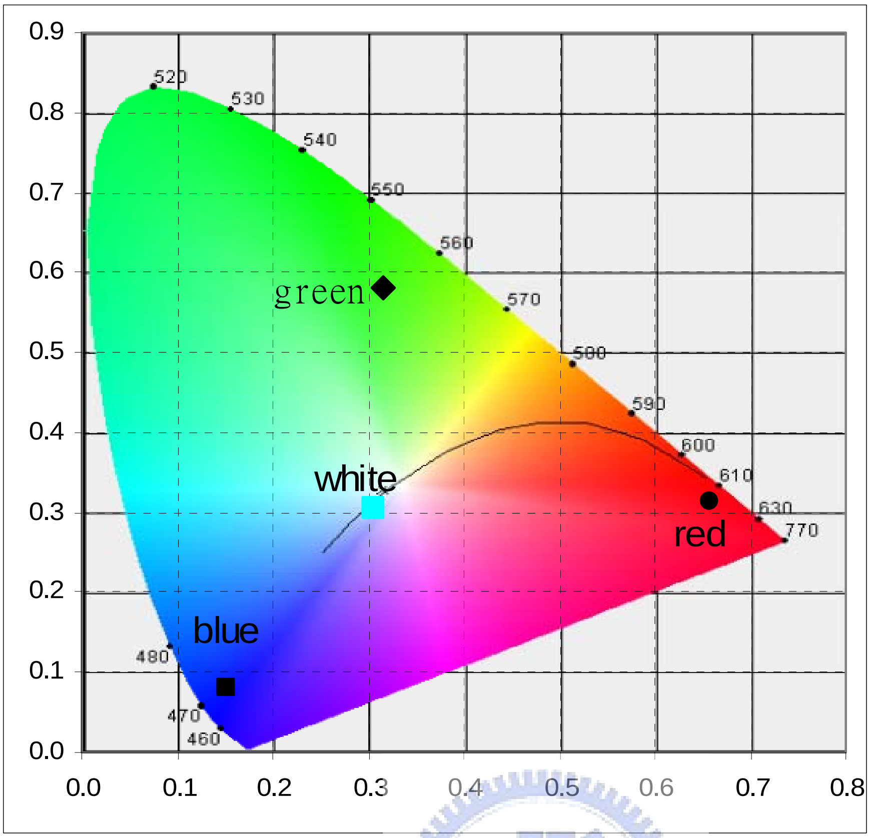

Fig. 3-14 The color coordinate of RGB color.

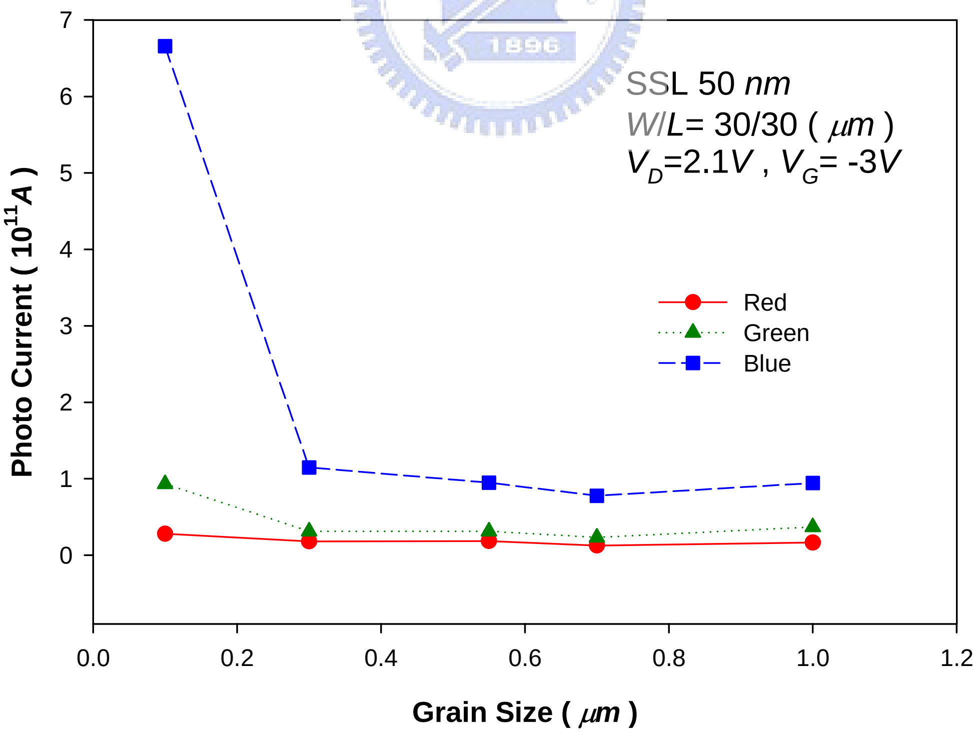

Fig. 3-15 Dependence of various grain size of photo leakage current with the illumination of RGB color. SSL device with the channel thickness 50*nm* at the V_{DS}=2.1*V* and V_{GS}= -3 *V* (*W*/ *L* = 30 μm/30 μm).

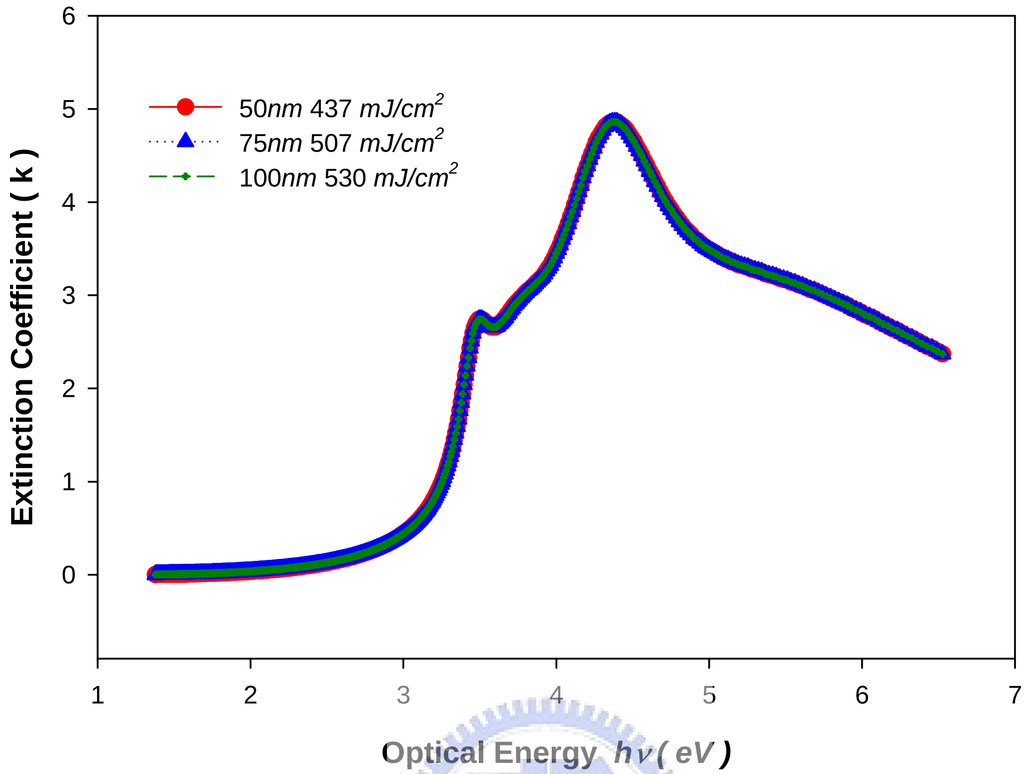

Fig. 3-16　Exitinction coefficient of different channel thickness.

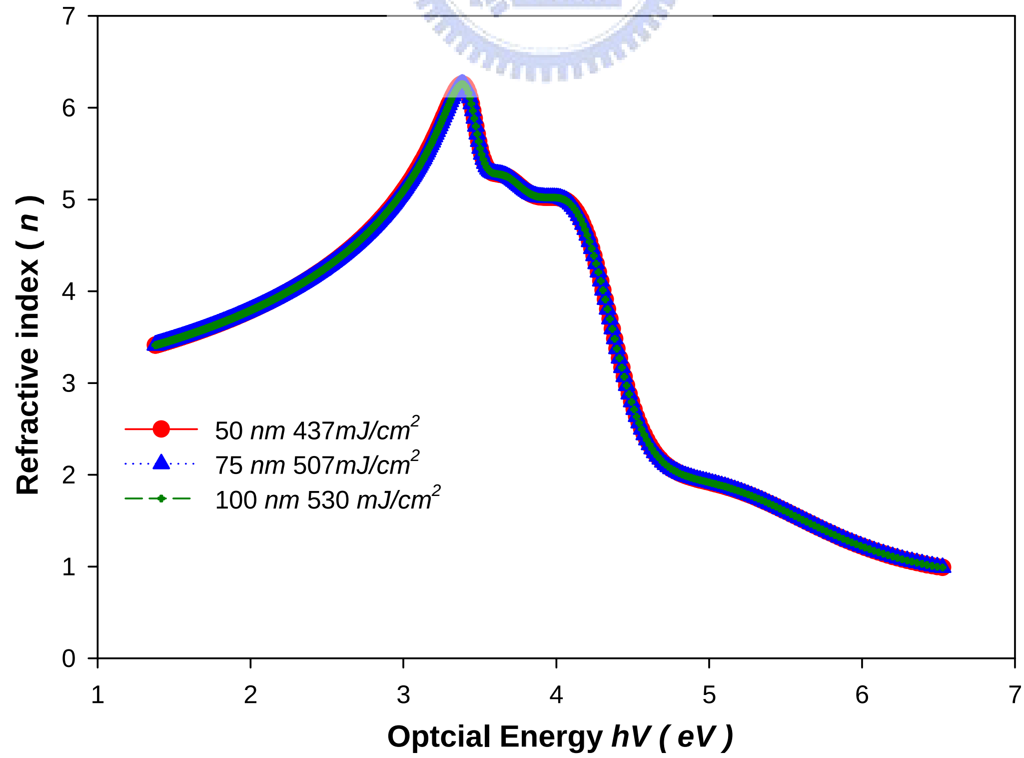

Fig. 3-17　Refractive index of different channel thickness.

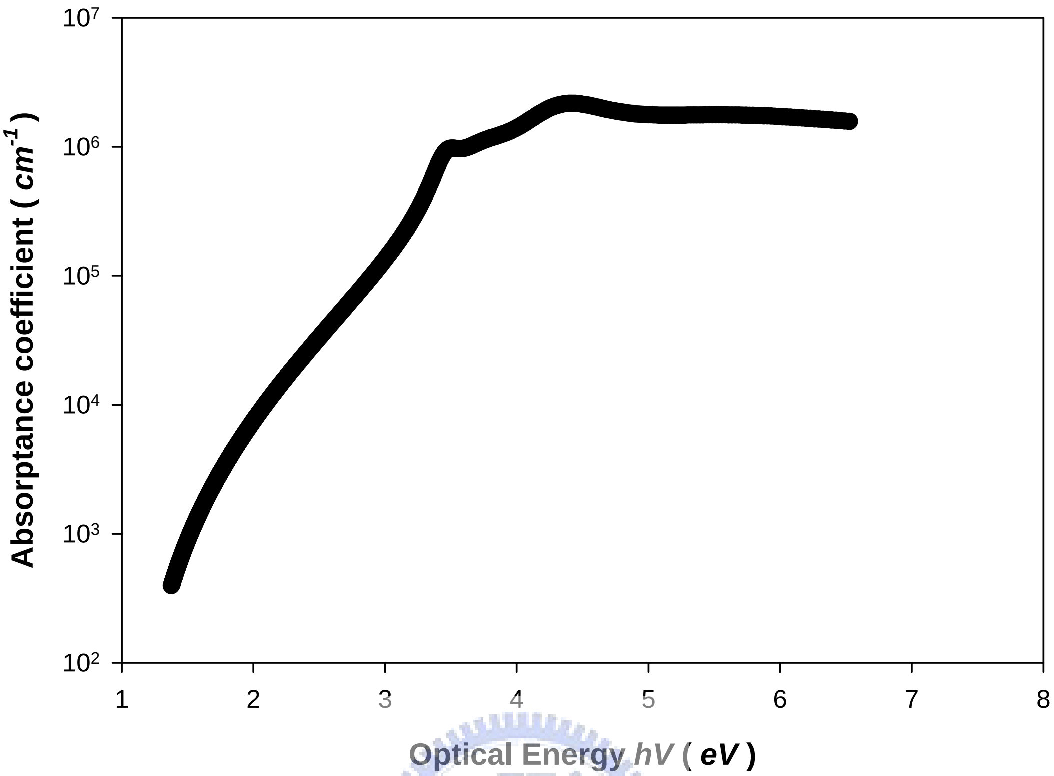

Fig. 3-18 Absorbtance coefficient of poly-Si film.

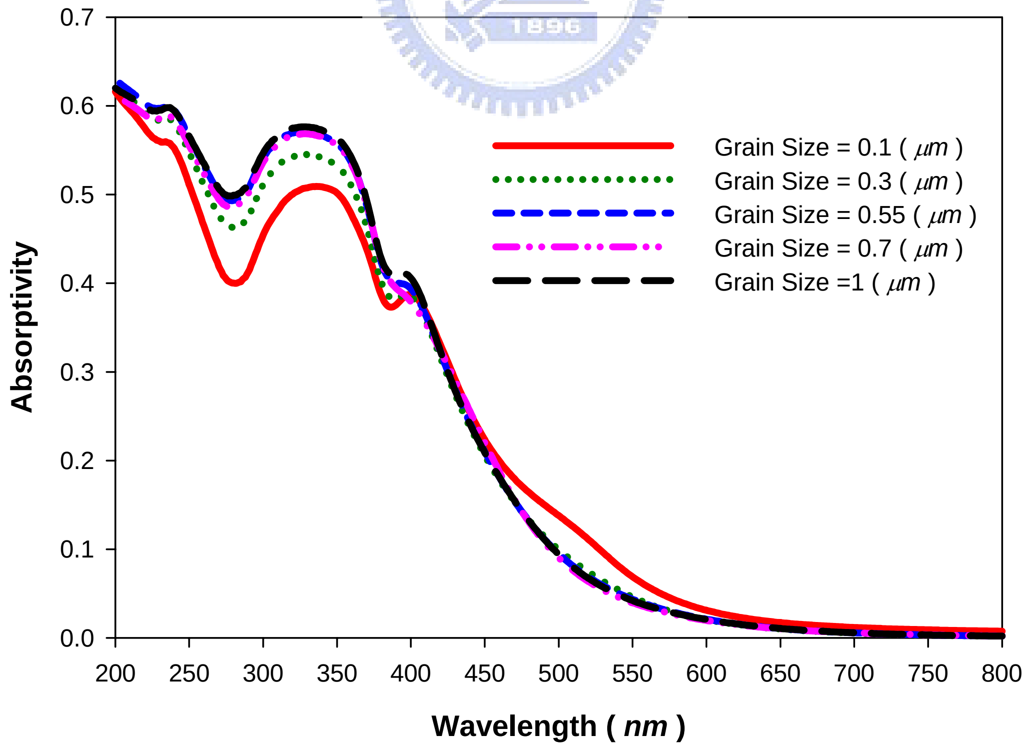

Fig.3-19 Absorptivity of the SSL films with different grain size at the channel thickness 50*nm*.

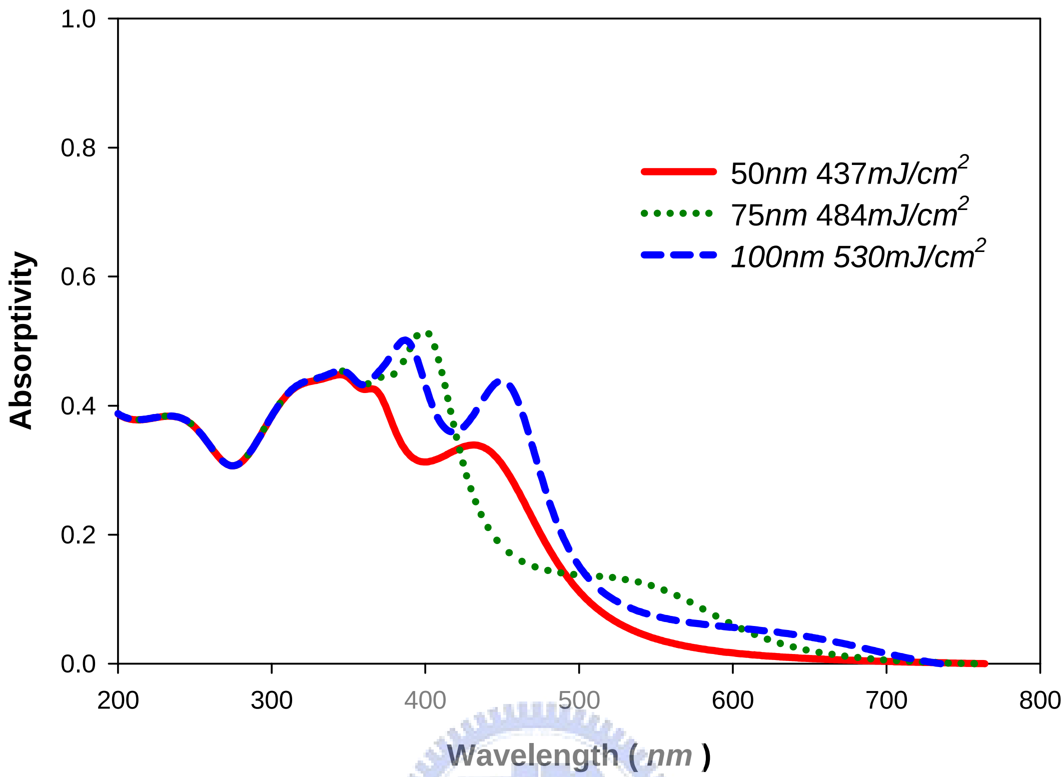

Fig.3-20 Absorptivity of the SSL films with different channel thickness.

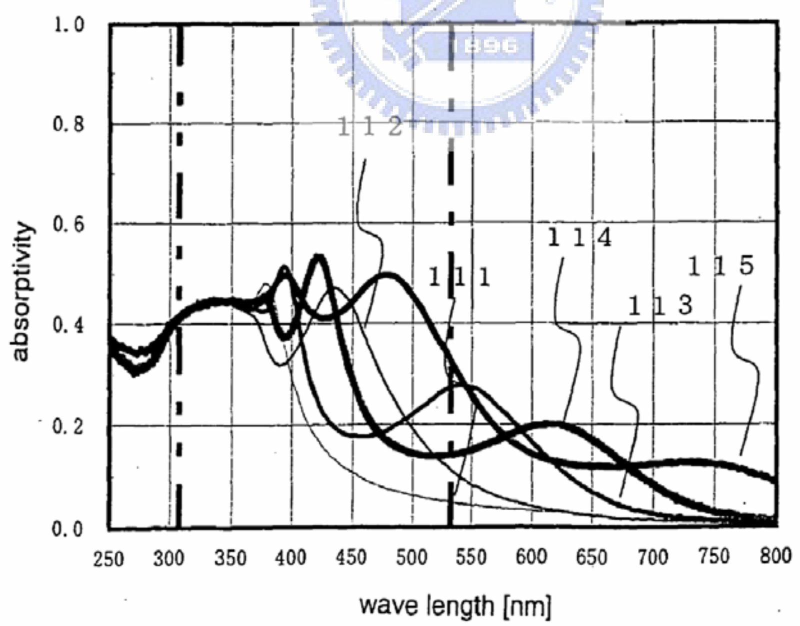

Fig. 3-21 Absorptivity of different channel thickness from ref [20].Where 111 、112、113、114、115 represent the channel thickness of 30*nm*、50 *nm*、70 *nm*、90 *nm* and 110 *nm* respectively.

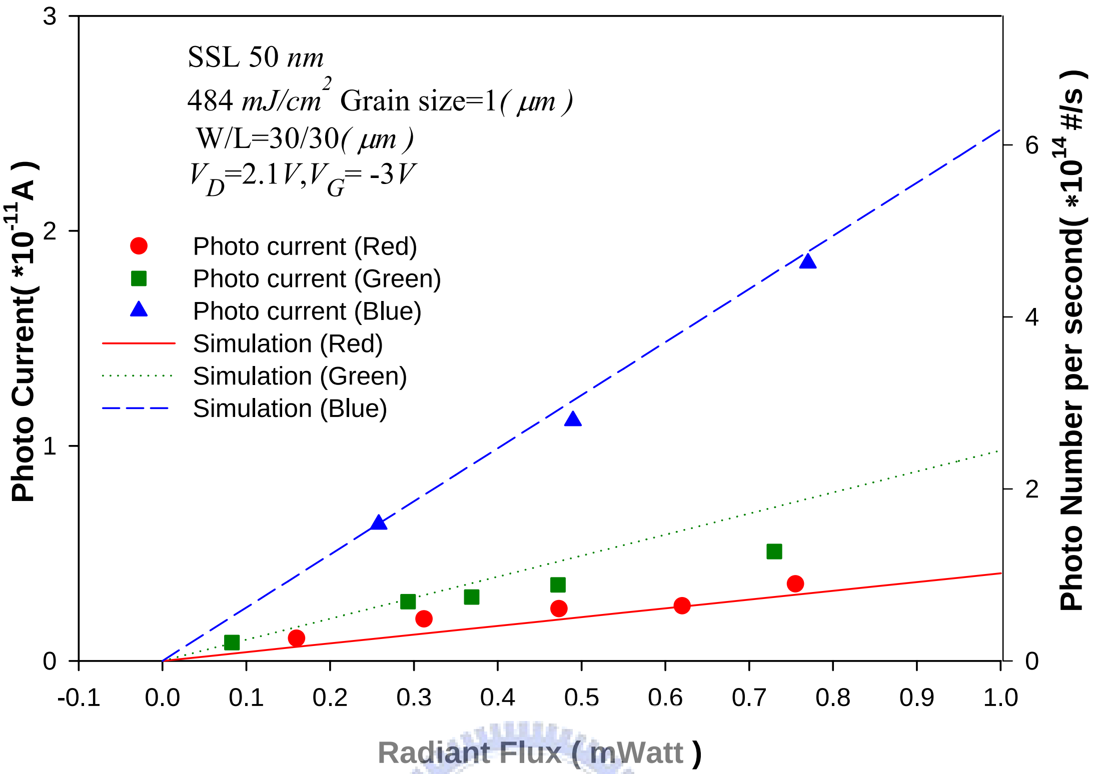

Fig. 3-22 Simulation of photon number per second with the illumination of different radiant flux. Compare with the photo leakage with the illumination of RGB color on the SSL device with the channel thickness 50*nm* and grain size=1*μm*. The lines represent the simulated result and the symbol represent the experimental data at the V_{DS}=2.1*V* and V_{GS}= -3 *V* (*W*/ *L* = 30 *μm*/30 *μm*).

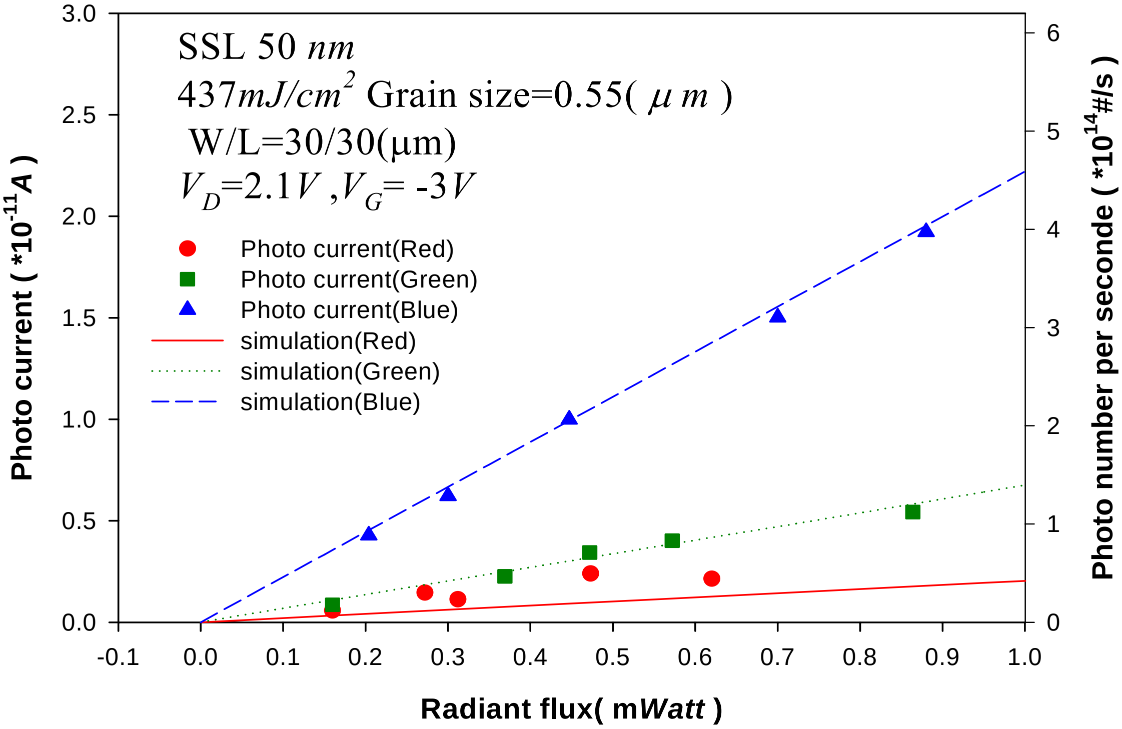

Fig. 3-23 Simulation of photon number per second with the illumination of different radiant flux. Compare with the photo leakage with the illumination of RGB color on the SSL device with the channel thickness 50*nm* and grain size=0.55*μm*. The lines represent the simulated result and the symbol represent the experimental data at the V_{DS}=2.1*V* and V_{GS}= -3 *V* (*W/ L = 30 μm/30 μm*).

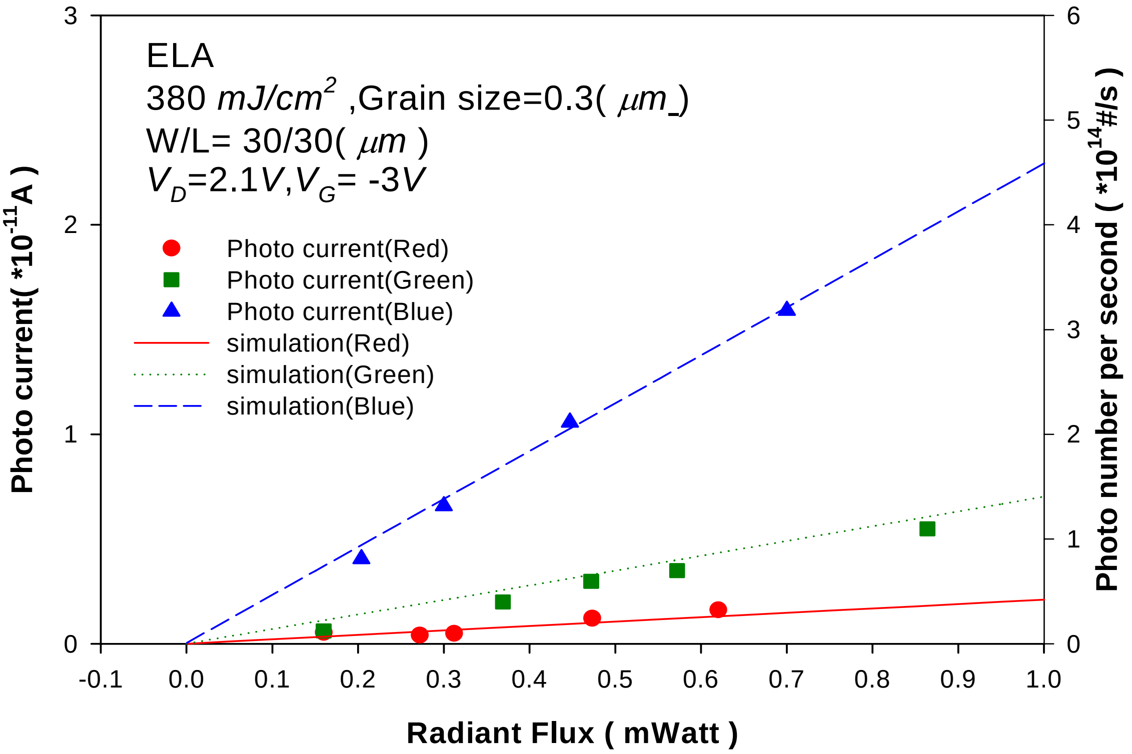

Fig. 3-24 Simulation of photon number per second with the illumination of different radiant flux. Compare with the photo leakage with the illumination of RGB color on the ELA device with the channel thickness 50*nm* and grain size=0.3 *μm*. The lines represent the simulated result and the symbol represent the experimental data at the V_{DS}=2.1*V* and V_{GS}= -3 *V* (*W*/ *L* = 30 *μm*/30 *μm*).